

Supporting Information for

Super-Resolution Imaging of Lysosomes with a Nitroso-Caged Rhodamine

Haihong He^a, Zhiwei Ye^b, Ying Zheng^b, Xiu Xu^a, Yi Xiao^{b,*}, Wei Yang^{b,*}, Xuhong Qian^{*a}, Youjun Yang^{a,*}
(H. He and Z. Ye contributed equally to this work.)

^a State Key Laboratory of Bioreactor Engineering, Shanghai Key Laboratory of Chemical Biology, School of Pharmacy, East China University of Science and Technology, 130 Meilong Road, Shanghai, China 200237.

^b State Key Laboratory of Fine Chemicals, Dalian University of Technology, 2 Linggong Road, Liaoning, China, 116024.

Page	Content
S2-3	General methods.
S4	Synthesis.
S5	Table S1. Crystal data and structure refinement for NOR535 .
S6	Table S2. Spectral and photophysical parameters of NOR535 and the corresponding rhodamine fluorophore in phosphate buffer (50 mM, pH = 7.4) with 1% DMSO as a co-solvent.
S7	Figure S1. The detection of NO released from NOR535 upon photolysis with 365 nm light.
S8	Figure S2. Dark stability of NOR535 (10 μM) without or with the presence of biological reductants. Figure S3. The pH titration of fluorophore 1 (10 μM) in water with 1% DMSO as a co-solvent.
S9	Figure S4. Spectral monitoring of the photolysis of NOR535 (10 μM) at 365 nm in (A) phosphate buffer (50 mM, pH = 7.4) and (B) citrate buffer (50 mM, pH = 4.7) with 1% DMSO in the presence of various indicated reducing agents (10 μM).
S10	Figure S5. Viability of HeLa cells toward NOR535 and 1 by MTT assay for 24 h. Figure S6. <i>In vivo</i> activation of NOR535 by mercury lamp equipped with a 330-385 nm filter and subsequent imaging of fluorophore 1 .
S11-S18	The ¹ H-NMR, ¹³ C-NMR and HRMS characteristics of all compounds.
S19	Supporting References.

General Methods

All chemicals and solvents were of analytical grades and used after redistilled. All $^1\text{H-NMR}$ and $^{13}\text{C-NMR}$ spectra were collected with a Bruker AV-400 spectrometer. Chemicals shifts were referenced to the residue solvent peaks and given in unit of ppm. ESI-HRMS spectra were acquired on a TOF mass spectrometer. UV-Vis absorption spectra were collected on a SHIMADZU UV-2600 UV-vis spectrophotometer. Fluorescence emission spectra were collected on a PTI-QM4 steady-state fluorimeter.

Spectroscopic methods. UV-Vis absorption spectra were acquired over a SHIMADZU UV-2600 spectrophotometer. Fluorescence spectra were collected on a PTI-QM4 steady-state fluorimeter, equipped with a 75 W Xeon arc lamp and a model 810 type PMT. Voltage of the PMT was set to 950 V. All spectra were collected with a 1-cm quartz cuvette (3.4 mL). Molar absorptivity was calculated with the Beer-Lambert law with absorption spectra of dilute solutions of each compound (O.D. < 0.05). Fluorescence quantum yields were calculated following literature procedures. Rhodamine B with a fluorescence quantum yield of 0.49 in ethanol was used as the reference.^[1]

Cell culture. HeLa (helicyon gartleri) cells were purchased from Cell Bank of Type Culture Collection of Chinese Academy of Sciences. The cells were all maintained in Dulbecco's modified Eagle's medium (DMEM, Gibco) supplemented with 10% fetal bovine serum (FBS, Hyclone). The cells were cultured in a humidified atmosphere of 5% CO_2 /95% air at 37 °C (CO_2 incubator, Thermo Scientific) and grown on 25 mm cover slips (Fisherbrand, 12-545-102) for 1–2 days to reach 70–90% confluency before use.

Colocalization imaging. HeLa cells were incubated with 10 μM **NOR535** for 5 min and 1 μM **Lysotracker Red** for 5 min sequentially and washed with PBS for three times to remove excess dyes. Confocal images were recorded on an Olympus FV1000 confocal microscope. Briefly, two lasers (488 nm for **NOR535** and 559 nm for **Lysotracker Red**) were sequentially applied for imaging to avoid emissive overlap between two dyes. Lasers were focused at the back focal plane of an UPLSAPO 100x oil objective. The fluorescence emission was filtered with a DM 405/488/559/635 and further separate to two channels with SDM 560. The wavelength selection performed by a galvanometer diffraction grating is used as following: 520-560 nm for **NOR535** and 570-610 nm for **Lysotracker Red**. The colocalization data was analyzed with the manufacturer's software.

Activation analysis. HeLa cells were stained with 10 μM **NOR535** for 5 min and then washed with PBS for three times. Firstly, a confocal image was recorded (ex: 448 nm; em: 520-560 nm) on an Olympus FV1000 confocal microscope. Then, UV irradiation from mercury lamp through 330-385 nm filter was used for activating **NOR535** to produce dye **1** and the activation images was collected under the same condition.

Single molecule localization microscopies. Imaging were performed on an Olympus IX71 inverted microscope. Two continuous laser (200 W, Coherent, Sapphire 532-200 and 100 W, Coherent, OBIS 405-100) were automatically controlled by an acousto-optic tunable filter (AOTF). These lasers were further transmitted through an optical fiber, adjusted by motorized-TIRFM illuminator and focused on the back focal plane of an Olympus UAPON 100xo TIRF objective (NA 1.49). The emission from samples was filtered through a Semrock

Di01-R405/488/532/635 filter and recorded on an Electron Multiplying CCD (Andor, 897U).

PALM imaging. HeLa cells were stained with 500 nM **NOR535** for 5 min and then washed with PBS for three times. The final imaging medium was RPMI 1640 without phenol red (Macgene) supplemented with 10% FBS (Hyclone).

The photoactivation laser for the super resolution imaging was 405 nm of 10 W/cm² and the imaging laser was 532 nm of ~2 kW/cm². A wide-field image was recorded with <1 W/cm² 532nm laser light. 3000 raw images were acquired at 100Hz.

Before PALM imaging, the cell was exposure to 10W/cm² 405 nm laser light to induce photolysis of NOR535 for 2 seconds. Then, a wide-field image was recorded with < 1W/cm² 532 nm laser light. During imaging, the sample was continually excited with a ~2 kW/cm² 532 nm laser. 3000 images were acquired at 100 Hz.

Single molecule analysis. Super resolution imaging analysis was performed in ThunderStorm^[2]. Briefly, the raw frames were filtered with difference-of-Gaussians filter to select the PSF candidates (For activation analysis, a B-Spline wavelet filter was used for evaluating the point spread functions (PSF) candidates). Then those PSFs were fitted with an integrated form of symmetric 2D Gaussian function (Fitting radius: 3.0 pixel) following Maximum likelihood method^[3,4] to gave the expected the precise location and single molecule intensity. The localization precision was calculated according to the Thompson formula^[5]. Those PSFs with too large width (> 1.3 x median(sigma)), too small width < 0.7 x median(sigma)) are eliminated.

The photons emitted from single molecule could be converted from single molecule intensity through the equation below:

$$\text{Photons} = (I_{\text{sig}} - I_{\text{bg}}) * \text{ADU} / (\text{QE} * \text{EMGAIN})$$

I_{sig} is the single molecule intensity from the fitting result. I_{bg} is the background intensity. ADU, the CCD sensitivity, and QE, the quantum efficiency of the camera, are read from the camera manufacturer's performance sheet. EMGAIN is the gain value used in the experiments (300 in this experiment).

3-Oxo-3H-spiro[isobenzofuran-1,9'-xanthene]-3',6'-diyl bis(trifluoromethanesulfonate) (3).^[6] **Fluorescein Sodium** (2.00 g, 5.32 mmol) was dissolved in anhydrous dichloromethane (50 mL) and cooled to 0°C. After addition of triethylamine (3.36 g, 42.52 mmol), trifluoromethanesulfonic anhydride (6.00 g, 21.26 mmol) was slowly added into the mixture, and the reaction was stirred for 4h from 0°C to room temperature. The reaction was terminated by water, and then extracted with DCM for 3 times, washed by saturated brine for 2 times, dried over anhydrous magnesium sulfate. Evaporation of the solvent resulted in a yellowish solid. The crude material was purified by flash column chromatography to yield the product as a white solid (2.80 g) in a 88% yield. ¹H-NMR (400 MHz, CDCl₃, δ): 8.08 (d, J = 7.1 Hz, 1H), 7.79-7.68 (m, 2H), 7.31 (d, J = 2.4 Hz, 2H), 7.20 (d, J = 7.4 Hz, 1H), 7.04 (dd, J₁ = 8.8 Hz, J₂ = 2.4 Hz, 2H), 6.97 (q, J = 8.8 Hz, 2H); ¹³C-NMR (101 MHz, CDCl₃, δ): 168.5, 152.1, 151.4, 150.2, 135.8, 130.7, 130.0, 125.7, 125.6, 123.8, 123.5, 120.3, 119.4, 117.7, 117.1, 113.9, 110.7, 80.1, 76.7.

3',6'-Bis((2-morpholinoethyl)amino)-3H-spiro[isobenzofuran-1,9'-xanthene]-3-one (1).^[6] Compound **2** (1.00 g, 1.68 mmol), 2-morpholinoethan-1-amine (0.52 g, 4.02 mmol), cesium carbonate (1.53 g, 4.69 mmol), Pd₂dba₃ (1% equivalent) and Xphos (1.5% equivalent) were dissolved in anhydrous 1,4-dioxane (80 mL), and then heated to 100°C for 8 h under argon protection. When the reaction was completed, the mixture was cooled to room temperature. After evaporation of the dioxane, water was added and the solution was extracted with DCM for 3 times, dried over anhydrous magnesium sulfate. Evaporation of the solvent resulted in a red solid. The crude material was purified by flash column chromatography to yield the product as a red solid (0.84 g) in a 90% yield. ¹H-NMR (400 MHz, CDCl₃, δ): 7.99 (d, J = 7.5 Hz, 1H), 7.66 – 7.56 (m, 2H), 7.17 (d, J = 7.5 Hz, 1H), 6.52 (d, J = 8.6 Hz, 2H), 6.40 (d, J = 2.2 Hz, 2H), 6.30 (dd, J₁ = 8.6 Hz, J₂ = 2.3 Hz, 2H), 4.58 (s, 2H), 3.72 (t, J = 4.6 Hz, 8H), 3.18 (t, J = 6.0 Hz, 4H), 2.64 (t, J = 5.9 Hz, 4H), 2.47 (m, 8H); ¹³C-NMR (101 MHz, CDCl₃, δ): 169.8, 153.1, 150.3, 134.6, 129.3, 128.9, 124.8, 124.0, 110.2, 107.6, 98.3, 66.9, 56.8, 53.3, 39.6.; HRMS (ESI) *m/z*: [M + H]⁺ calculated for C₃₂H₃₇N₄O₅⁺, 557.2764; found, 557.2767.

N,N'-(3-oxo-3H-spiro[isobenzofuran-1,9'-xanthene]-3',6'-diyl)bis(N-(2-morpholinoethyl)nitrous amide) (NOR535). Compound **1** (400 mg, 0.72 mmol) was dissolved in a solution mixture of dichloromethane and acetic acid (20 mL, v/v=10:1) and cooled to 0°C. Added NaNO₂ (500 mg, 7.19 mmol) in portion and reacted at room temperature. The reaction mixture was neutralized with saturated NaHCO₃ aqueous solution and extracted with dichloromethane 3 times, dried over magnesium sulfate. Evaporation of the solvent resulted in solid. The crude material was purified by flash column chromatography to yield the product as a orange pale solid (420 mg) in a 95% yield. ¹H-NMR (400 MHz, CDCl₃, δ): 8.10 (d, J = 7.1 Hz, 1H), 7.74 (td, J₁ = 7.28 Hz, J₂ = 1.2 Hz, 1H), 7.70 (td, J₁ = 7.52 Hz, J₂ = 1.2 Hz, 1H), 7.64 (d, J = 2.2 Hz, 2H), 7.38 (dd, J₁ = 8.7 Hz, J₂ = 2.2 Hz, 2H), 7.23 (d, J = 7.3 Hz, 1H), 6.97 (d, J = 8.7 Hz, 2H), 4.15 (t, J = 6.6 Hz, 4H), 3.66 (t, J = 4.6 Hz, 8H), 2.51 – 2.47 (m, 12H); ¹³C-NMR (101 MHz, CDCl₃, δ): 169.0, 152.7, 151.6, 143.8, 135.5, 130.4, 129.3, 126.1, 125.5, 123.8, 117.4, 115.3, 107.9, 81.3, 77.3, 66.9, 54.4, 53.7, 41.5; HRMS (ESI) *m/z*: [M + H]⁺ calculated for C₃₂H₃₅N₆O₇⁺, 615.2562; found, 615.2565.

Table S1. Crystal data and structure refinement for **NOR535**.

Identification code	mo_d8v17076_0m	
Empirical formula	C33 H34 Cl2 N6 O7	
Formula weight	697.56	
Temperature	301.83 K	
Wavelength	0.71073 Å	
Crystal system	Triclinic	
Space group	P-1	
Unit cell dimensions	a = 11.1425(3) Å	a = 100.4860(10)°.
	b = 11.9013(4) Å	b = 92.7810(10)°.
	c = 13.4239(4) Å	g = 103.2090(10)°.
Volume	1696.54(9) Å ³	
Z	2	
Density (calculated)	1.366 Mg/m ³	
Absorption coefficient	0.248 mm ⁻¹	
F(000)	728	
Crystal size	0.12 x 0.08 x 0.05 mm ³	
Theta range for data collection	1.550 to 25.500°.	
Index ranges	-13<=h<=13, -14<=k<=14, -16<=l<=16	
Reflections collected	33344	
Independent reflections	6213 [R(int) = 0.0353]	
Completeness to theta = 25.242°	98.3 %	
Absorption correction	Semi-empirical from equivalents	
Max. and min. transmission	0.7458 and 0.6972	
Refinement method	Full-matrix least-squares on F ²	
Data / restraints / parameters	6213 / 0 / 433	
Goodness-of-fit on F ²	1.055	
Final R indices [I>2sigma(I)]	R1 = 0.0876, wR2 = 0.2241	
R indices (all data)	R1 = 0.1101, wR2 = 0.2455	
Extinction coefficient	n/a	
Largest diff. peak and hole	0.838 and -0.717 e.Å ⁻³	

Table S2. Spectral and photophysical parameters of **NOR535** and the corresponding rhodamine fluorophore in buffer with 5% DMSO as a co-solvent.

Compound	λ_{abs} (nm)	ϵ ($\text{cm}^{-1}\cdot\text{M}^{-1}$)	λ_{em} (nm)	ϕ
NOR535^a	305	11600	n.d.	n.d.
1^a	520	88000	550	0.09
NOR535^b	305	10300	n.d.	n.d.
1^b	510	92900	535	0.97
	480	36900		

^ain phosphate buffer (50 mM, pH = 7.4); ^bin citrate buffer (50 mM, pH = 4.7). Note: "n.d." stands for not-detected.

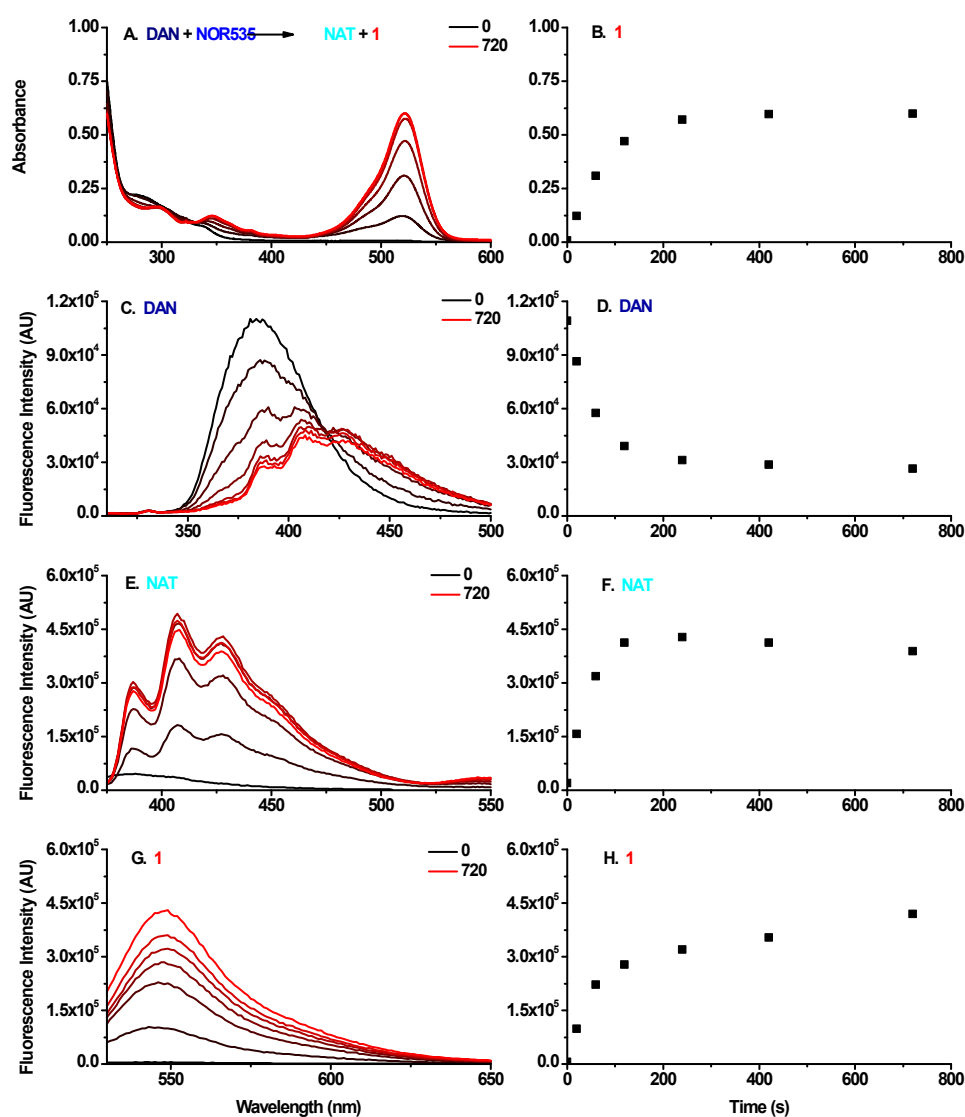


Figure S1. The detection of NO released from **NOR535** upon photolysis with 365 nm light. (A). Absorption signal of a solution containing **NOR535** (10 μM) and **DAN** (10 μM) in aqueous phosphate buffer (50 mM, pH = 7.4) with 5% DMSO upon photo-irradiation at 365 nm. (B). The gradual change of absorbance at 520 nm of the solution is plotted with respect to the duration of photo-irradiation. (C). Spectroscopic monitoring of the disappearance of **DAN** upon excitation at 300 nm. (D). The gradual change of emission intensity at 390 nm of **DAN** is plotted with respect to the duration of photo-irradiation, $\lambda_{\text{ex}} = 300$ nm. (E). Spectroscopic monitoring of the formation of **NAT** upon excitation at 365 nm. (F). The gradual change of emission intensity at 435 nm of **NAT** is plotted with respect to the duration of photo-irradiation, $\lambda_{\text{ex}} = 365$ nm. (G). Spectroscopic monitoring of the formation of **1** upon excitation at 515 nm. (H). The gradual change of emission intensity at 550 nm of **1** is plotted with respect to the duration of photo-irradiation, $\lambda_{\text{ex}} = 515$ nm.

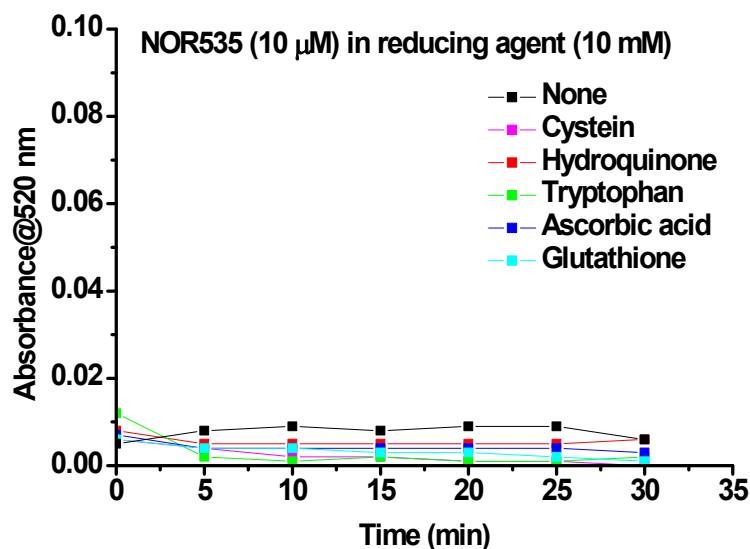


Figure S2. Dark stability of **NOR535** ($10\ \mu\text{M}$) without or with the presence of biological reductants [Cysteine ($10\ \text{mM}$), Hydroquinone ($10\ \text{mM}$), Tryptophan ($10\ \text{mM}$), Ascorbic acid ($10\ \text{mM}$) and GSH ($10\ \text{mM}$) in phosphate buffer ($50\ \text{mM}$, $\text{pH} = 7.4$) with 1% DMSO as a co-solvent]. The fluorescence intensity is collected at $520\ \text{nm}$.

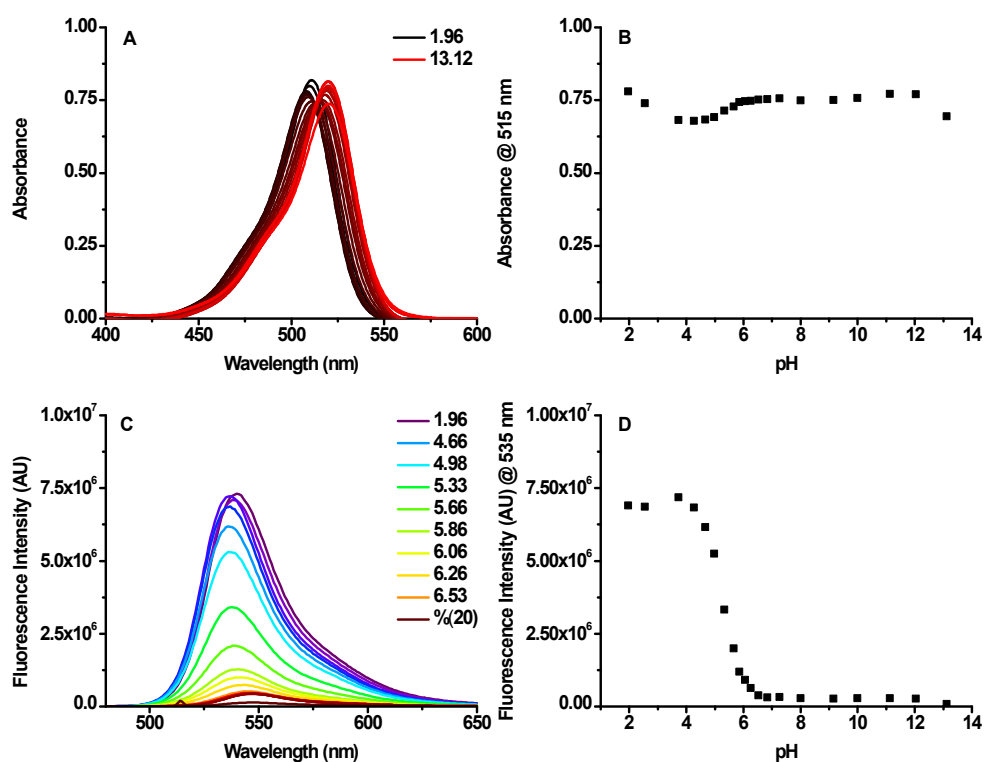


Figure S3. The pH titration of fluorophore **1** ($10\ \mu\text{M}$) in water with 1% DMSO as a co-solvent. (A) The absorption spectra of **NOR535** in different pH value. (B) The absorption at $515\ \text{nm}$ of **NOR535** in different pH value. (C) The emission spectra of **NOR535** in different pH value, $\lambda_{\text{ex}} = 515\ \text{nm}$. (D) The fluorescence intensity at $535\ \text{nm}$ of **NOR535** in different pH value, $\lambda_{\text{ex}} = 515\ \text{nm}$.

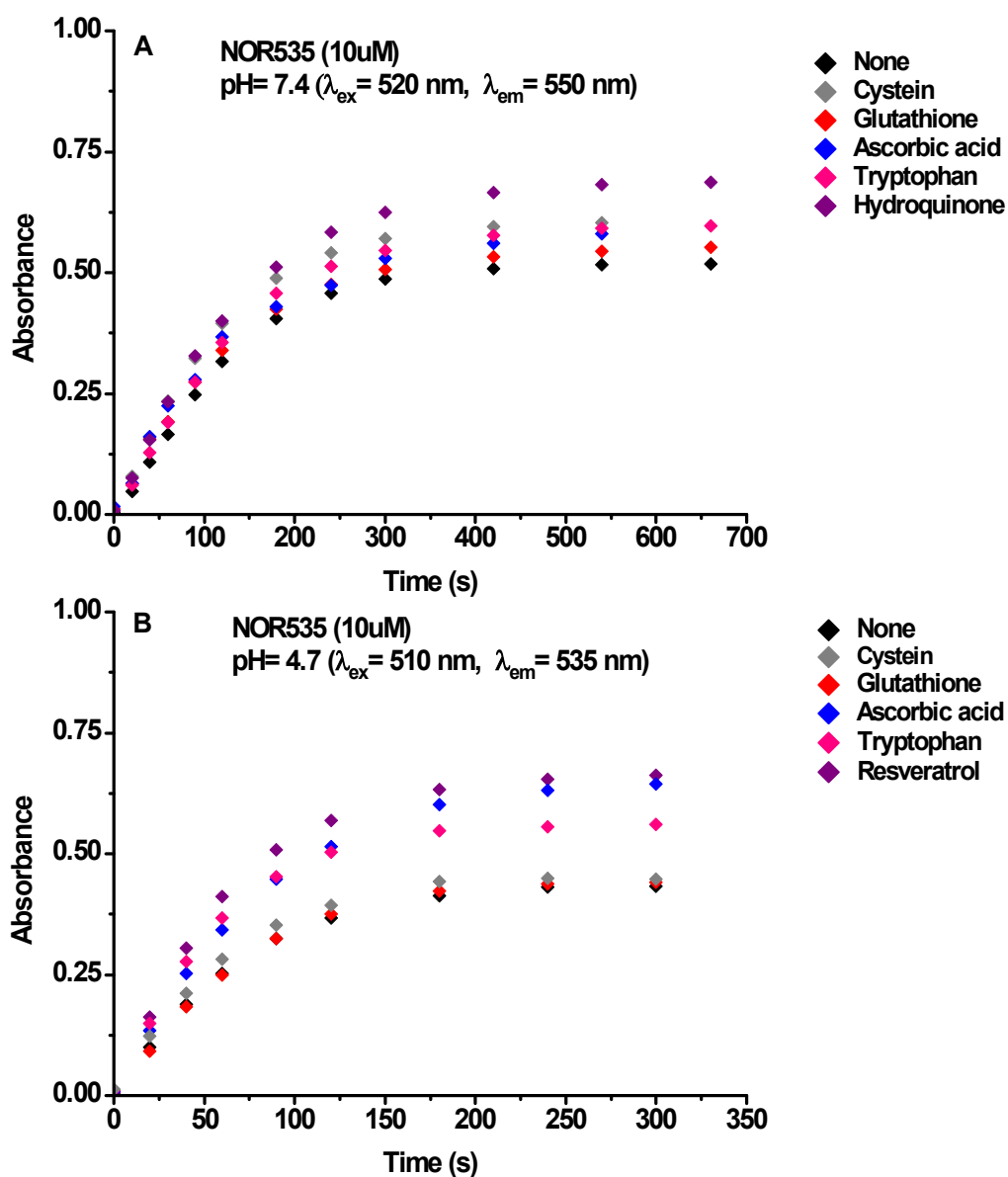


Figure S4. Spectral monitoring of the photolysis of **NOR535** (10 μM) at 365 nm in (A) phosphate buffer (50 mM, pH = 7.4) and (B) citrate buffer (50 mM, pH = 4.7) with 1% DMSO in the presence of various indicated reducing agents (10 μM).

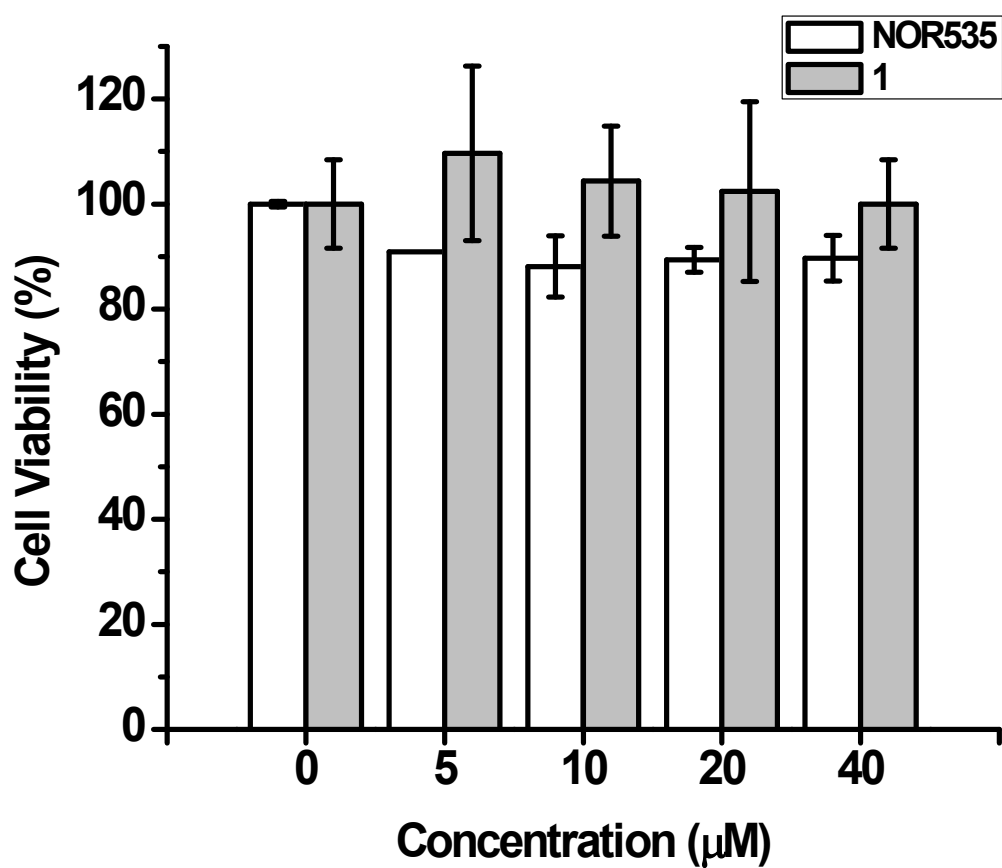


Figure S5. Viability of HeLa cells toward **NOR535** and **1** by MTT assay for 24 h.

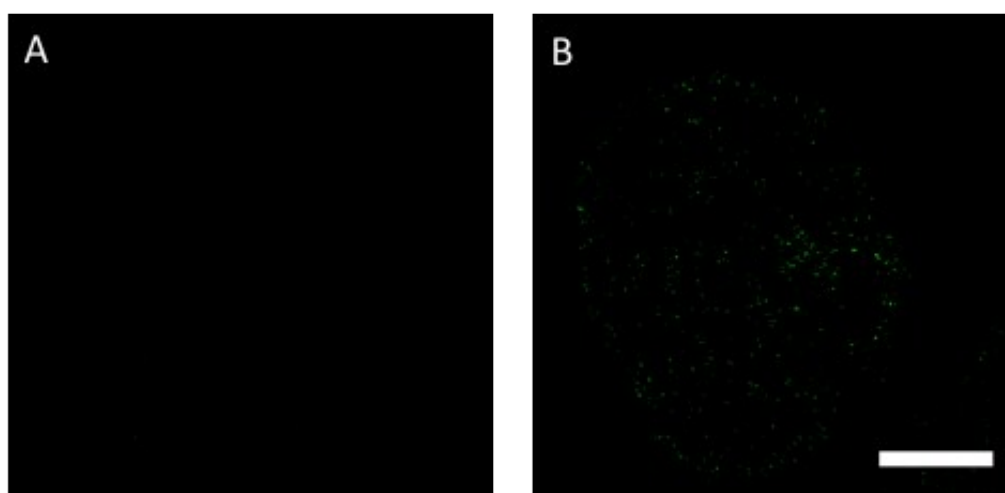


Figure S6. In vivo activation of **NOR535** by mercury lamp equipped with a 330-385 nm filter and subsequent imaging of fluorophore **1**. (A). Before activation. (B). After activation. Ex: 488 nm, em: 520-560 nm. Scale bar: 30 µm.

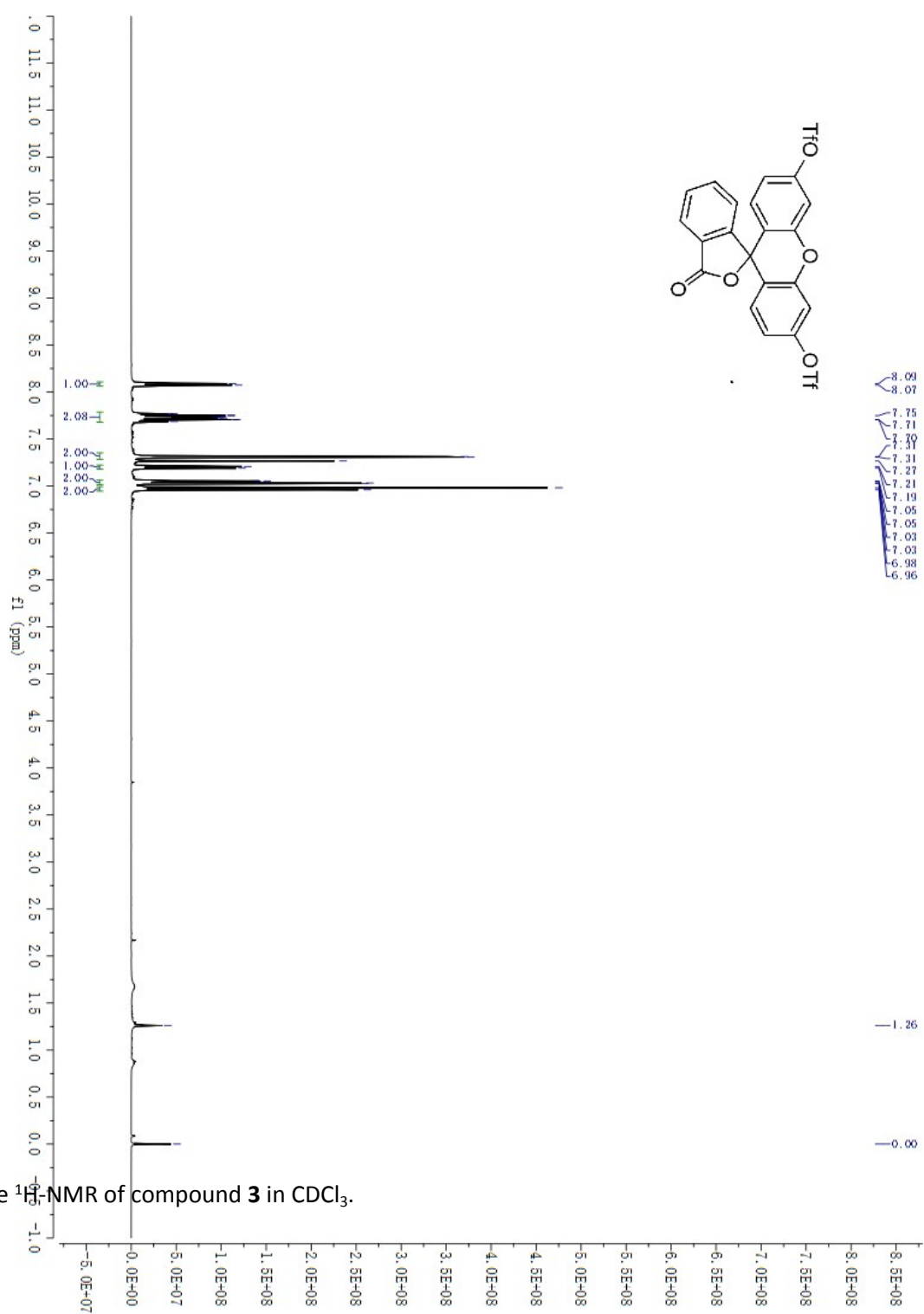


Figure S7. The ^1H NMR of compound **3** in CDCl_3 .

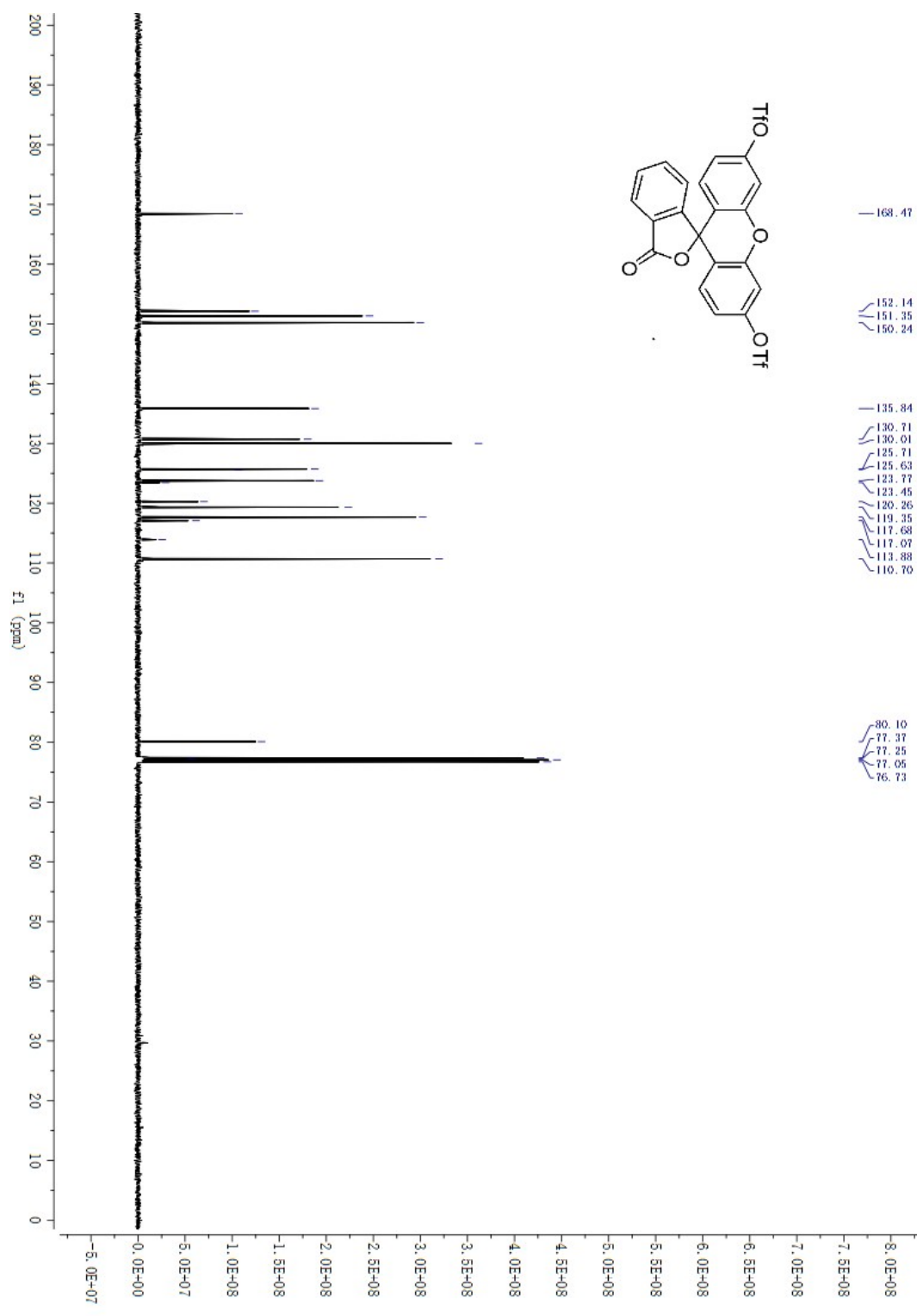


Figure S8. The ¹³C-NMR of compound 3 in CDCl₃.

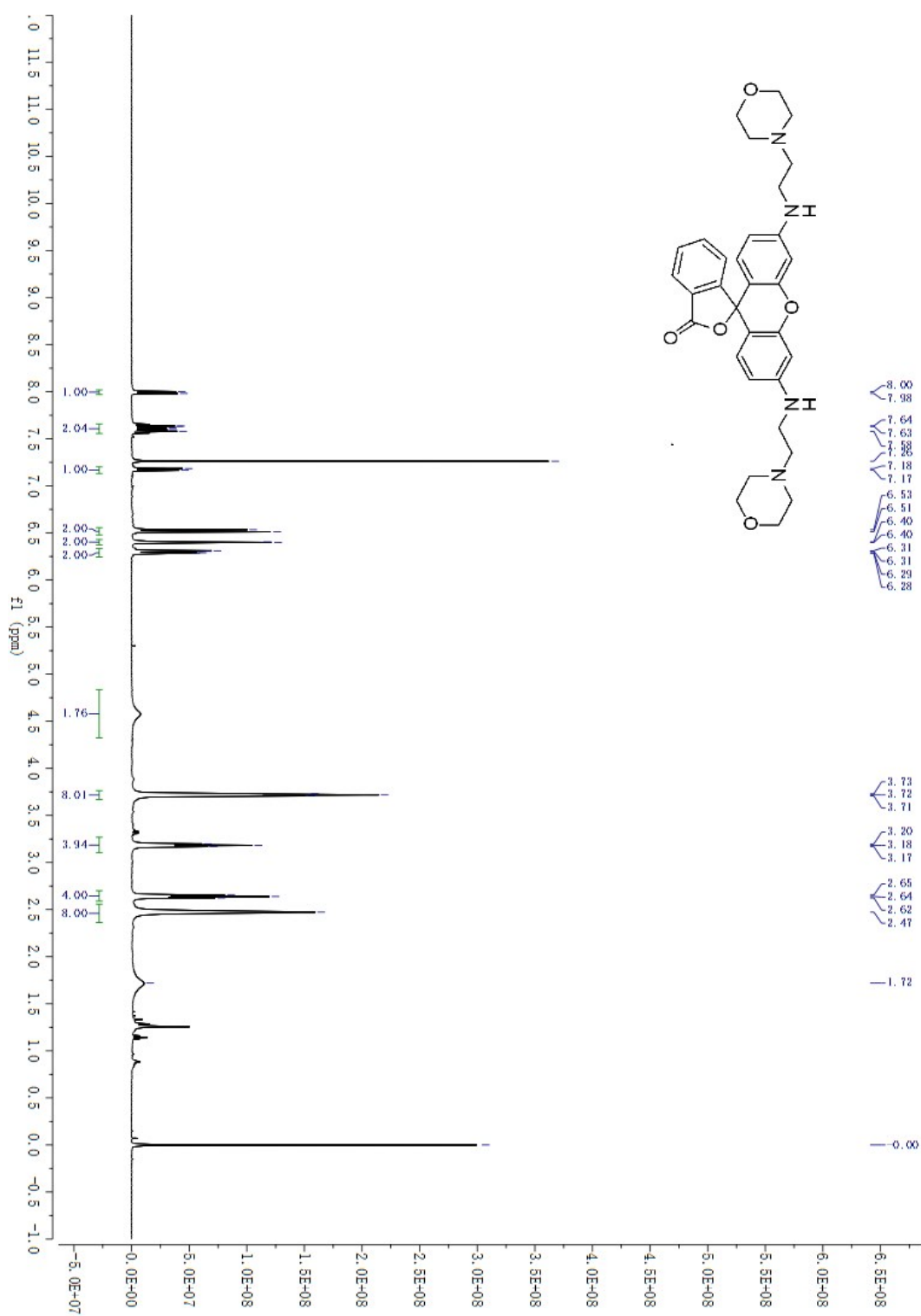


Figure S9. The ^1H -NMR of compound **1** in CDCl_3 .

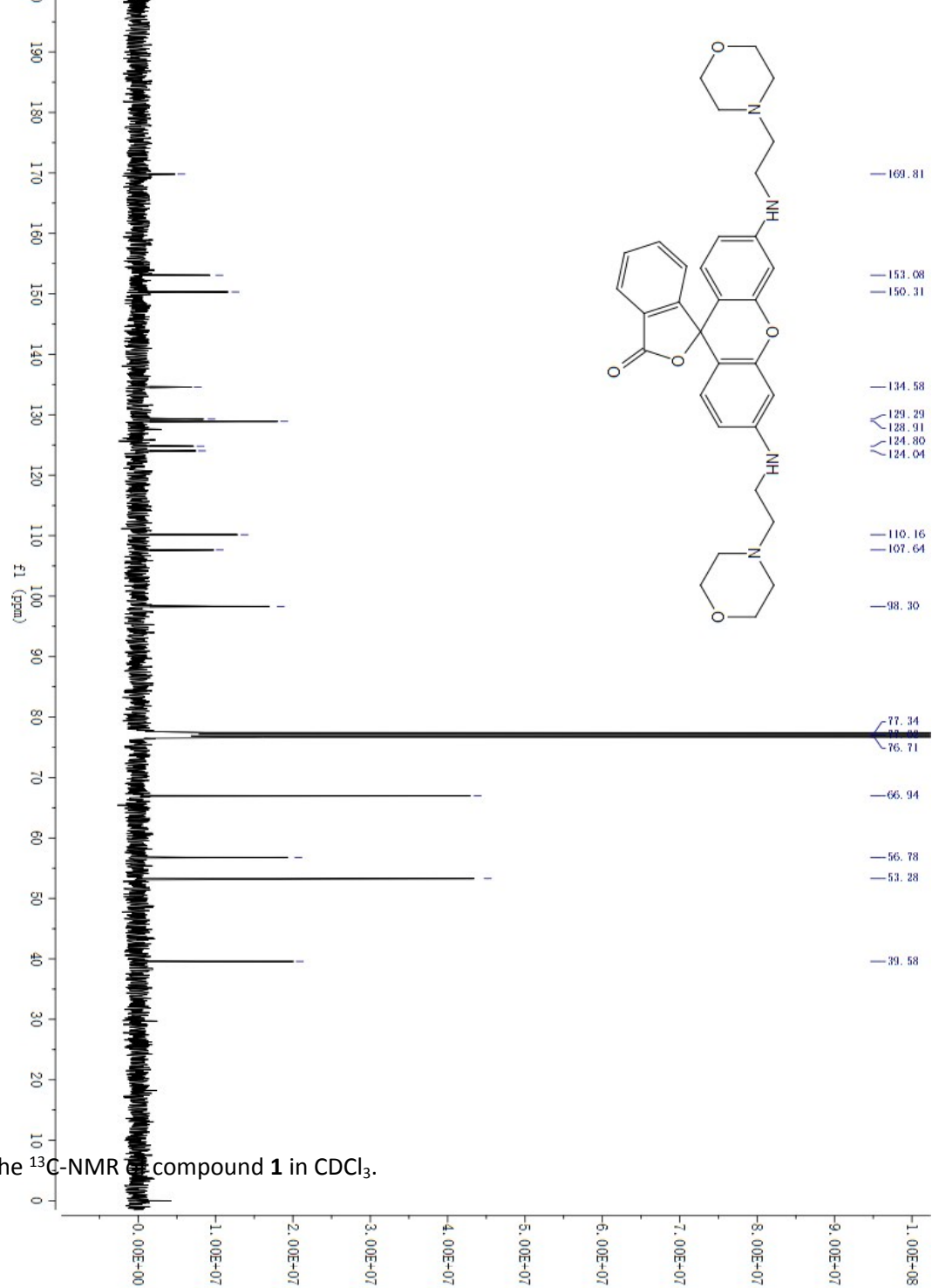


Figure S10. The ^{13}C -NMR of compound **1** in CDCl_3 .

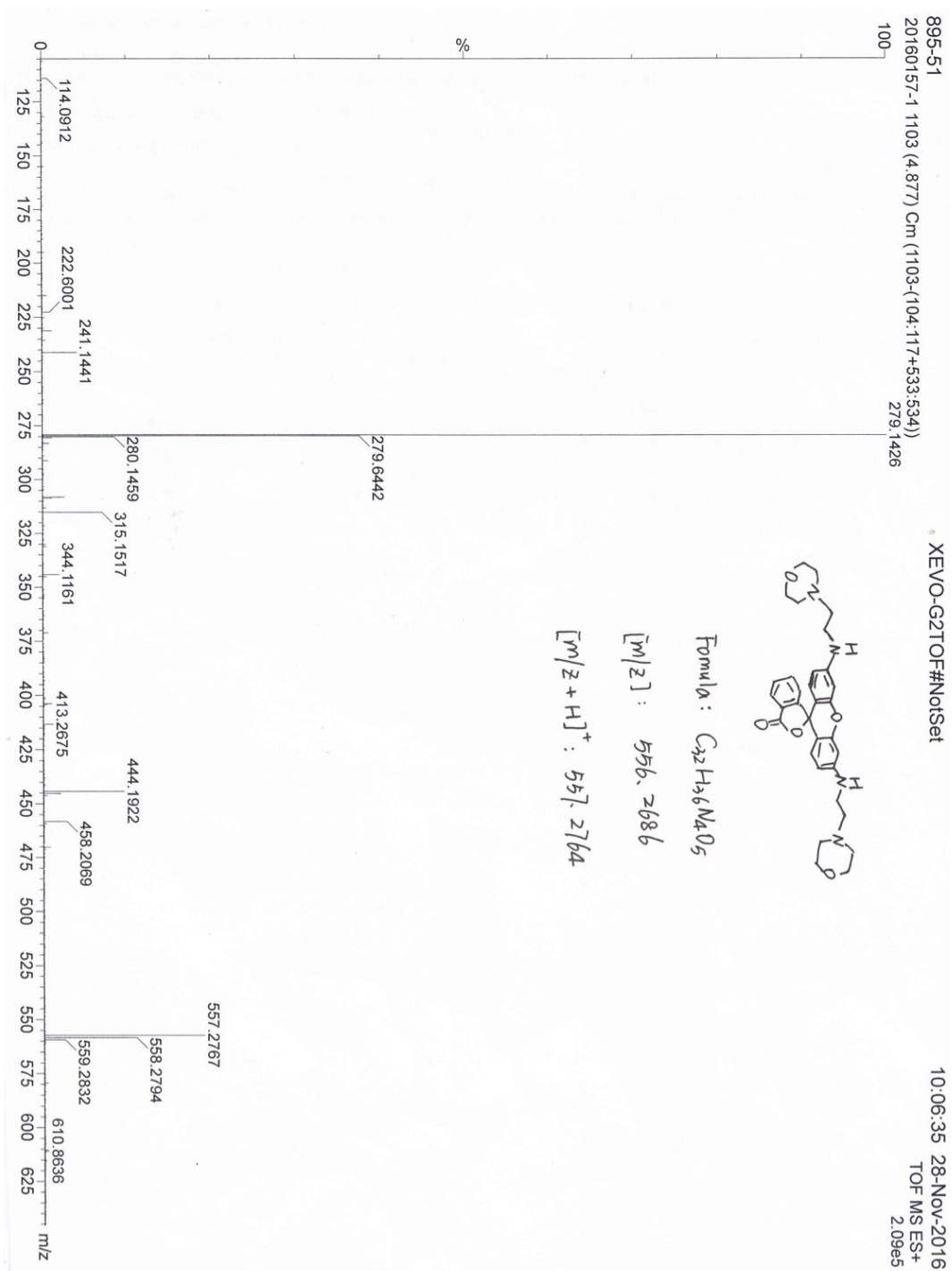


Figure S11. The HRMS of compound 1.

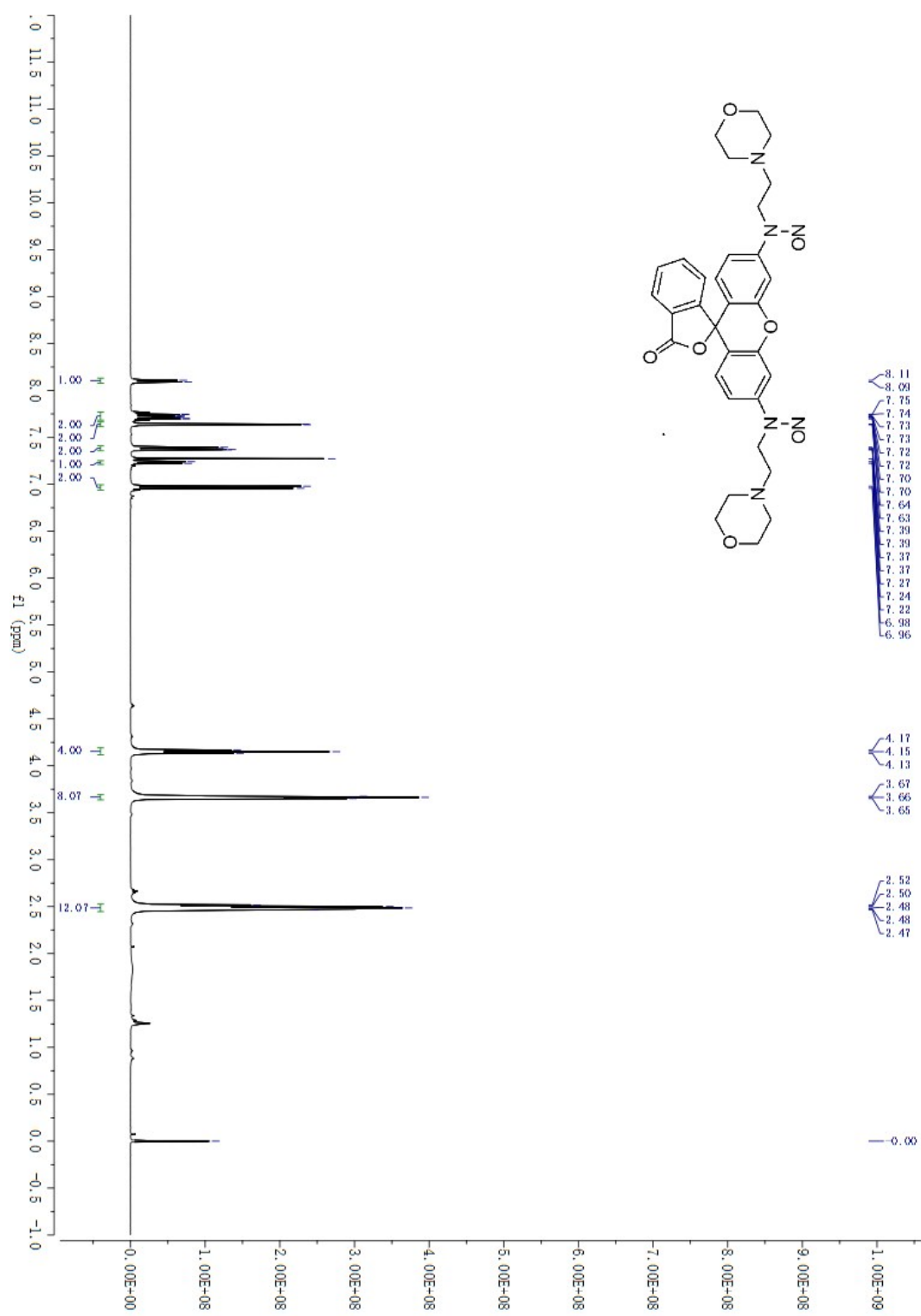


Figure S12. The ¹H-NMR of compound NOR535 in CDCl₃.

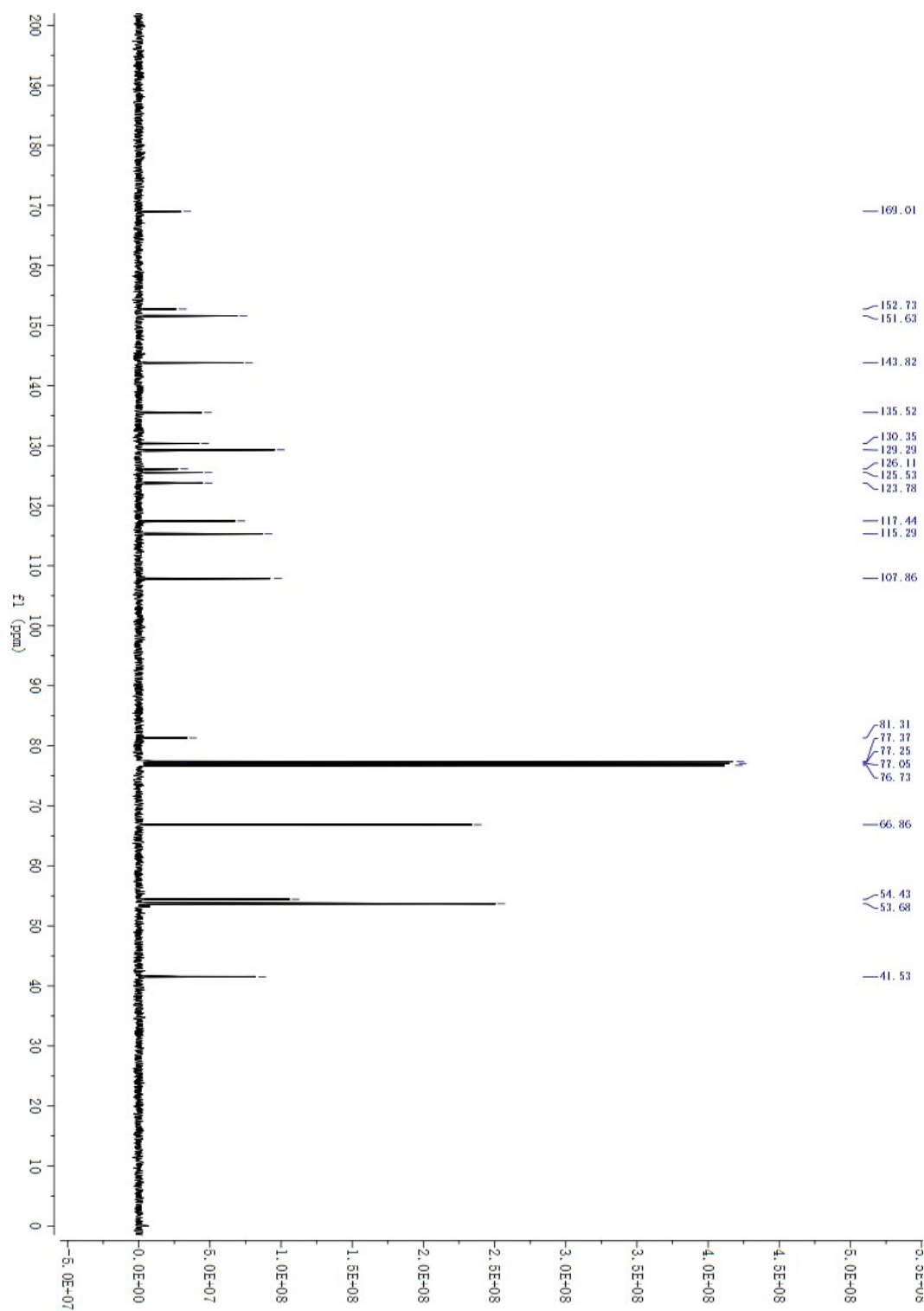


Figure S13. The ^{13}C -NMR of compound **NOR535** in CDCl_3 .

Supporting References

1. K. G. Casey and E. L. Quitevis, *J. Phys. Chem.*, 1988, **92**, 6590–6594.
2. M. Ovesný, P. Křížek, J. Borkovec, Z. Švindrych, and G. M. Hagen, *Bioinformatics*, 2014, **30**, 2389–2390.
3. K. I. Mortensen, L. S. Churchman, J. a Spudich, and H. Flyvbjerg, *Nat. Methods*, 2010, **7**, 377–381.
4. C. S. Smith, N. Joseph, B. Rieger, and K. A. Lidke, *Nat. Methods*, 2010, **7**, 373.
5. R. E. Thompson, D. R. Larson, and W. W. Webb, *Biophys. J.*, 2002, **82**, 2775–2783.
6. J. B. Grimm and L. D. Lavis, *Org. Lett.*, 2011, **13**, 6354–6357.